

Journal of Materials Chemistry A

Accepted Manuscript



This is an *Accepted Manuscript*, which has been through the Royal Society of Chemistry peer review process and has been accepted for publication.

Accepted Manuscripts are published online shortly after acceptance, before technical editing, formatting and proof reading. Using this free service, authors can make their results available to the community, in citable form, before we publish the edited article. We will replace this *Accepted Manuscript* with the edited and formatted *Advance Article* as soon as it is available.

You can find more information about *Accepted Manuscripts* in the [Information for Authors](#).

Please note that technical editing may introduce minor changes to the text and/or graphics, which may alter content. The journal's standard [Terms & Conditions](#) and the [Ethical guidelines](#) still apply. In no event shall the Royal Society of Chemistry be held responsible for any errors or omissions in this *Accepted Manuscript* or any consequences arising from the use of any information it contains.

MIL-101(Fe) as a Lithium-ion Battery Electrode Material: Relaxation and Intercalation Mechanism During Lithium Insertion

JaeWook Shin,^a Min Kim,^b ^{||} Jordi Cirera,^b Shawn Chen,^a Gregory J. Halder,^c Thomas A. Yersak,^a Francesco Paesani,^b Seth M. Cohen,^b and Ying Shirley Meng^{a*}

^aDepartment of Nanoengineering and ^bDepartment of Chemistry and Biochemistry, University of California, San Diego, La Jolla, California 92093, United States

^cX-ray Science Division, Advanced Photon Source, Argonne National Laboratory, Argonne, Illinois 60439, United States

^{||} Present address: Department of Chemistry, Chungbuk National University, 1 Chungdae-ro, Seowon-gu, Cheongju-si, Republic of Korea, 362-763

*Corresponding author Tel.: +1 8588224247, Fax: +1 8585349553

Email address: shmeng@ucsd.edu

Abstract

The electrochemical performance of the MIL-101(Fe) metal-organic framework (MOF) as a lithium ion battery electrode is reported for the first time. The iron metal centers can be electrochemically activated. The $\text{Fe}^{3+}/\text{Fe}^{2+}$ redox couple is electrochemically active, but not reversible over many cycles. A comparison between *ex-situ* and *in-operando* X-ray absorption spectroscopy (XAS) on the Fe K-edge is presented. Our results indicate that the capacity fade is related to a time dependent, irreversible oxidation of Fe^{2+} to Fe^{3+} . These results are key in proving the importance of *in-operando* XAS measurements. The MOF side reaction with the electrolyte has been computationally modeled. These results provide further insights on the mechanism responsible for the MOF lack of reversibility. Future guidelines for improving the reversibility of MOFs used as electrodes in Li-ion batteries based on the fine-tuning of the electronic structure of the material are proposed.

Keywords: Lithium ion battery, metal-organic frameworks, synchrotron, powder X-ray diffraction, X-ray absorption spectroscopy, electronic structure, density functional theory

Introduction

Rechargeable Li-ion batteries are essential for the development of smartphones, laptop computers, and many other technologies including grid energy storage.¹ The materials used in commercial Li-ion batteries are far too expensive and energy intensive for large-scale grid storage applications.¹⁻⁴ For example, layered oxide cathode materials are costly because they require a high temperature synthesis process and contain expensive transition metals like Co.⁵⁻⁸ In order to reduce the cost of Li-ion batteries for grid scale applications, metal-organic framework (MOF) cathode materials could be utilized. MOF materials offer several advantages with respect to other porous materials because of their flexible synthetic routes, low temperature synthesis, and comparatively inexpensive precursor materials.⁹

MOFs represent a relatively new class of porous materials assembled from two main components: an inorganic secondary building unit (SBU) and an organic linker.¹⁰ The SBUs are generally comprised of transition metal ions or small metal clusters, while the organic linkers include a wide range of molecules, such as dicarboxylates, with 1,4-benzene dicarboxylic acid (H₂bdc) being among the most commonly utilized ligands.¹¹ The Zn₄O(4,4',4''-benzene-1,3,5-triyl-tri-benzoate)₂ (MOF-177) was the first MOF to be studied as a host for lithium insertion.¹² Unfortunately, MOF-177 does not exhibit good electrochemical reversibility. Shortly after this initial study, two Fe³⁺-based MOFs – Fe(OH)_{0.8}F_{0.2}(bdc) (MIL-53(Fe)) and FeOH(bdc) (MIL-68(Fe), MIL = Materials of Institut Lavoisier) – were synthesized and tested as battery materials.^{13, 14} MIL-53(Fe) exhibits good electrochemical reversibility and was found to be superior to MIL-68(Fe).^{14,15} However, the synthesis of MIL-53(Fe) requires HF, which limits its potential as a large scale grid storage battery material. To avoid the use of HF, MIL-101(Fe) was chosen as an electrode candidate. The MIL-101(Fe) SBU is composed of a carboxylate-bridged, oxo-centered, trinuclear Fe³⁺ complex (Figure 1a). This particular SBU complex is a well-known motif in inorganic

chemistry, and its electron density distribution, magnetic, and electrochemical properties have been previously reported.¹⁵⁻¹⁷ The theoretical capacity of the material with one lithium insertion per Fe atom is 107.74 mAh g⁻¹.

Using powder X-ray diffraction (PXRD) and X-ray absorption spectroscopy (XAS), we find that MIL-101(Fe) undergoes structurally reversible intercalation reactions, with the Fe³⁺/Fe²⁺ redox couple being electrochemically active. However, in long term cycling, we observe an exponential decay in reversible lithium insertion capacity. To evaluate the irreversibility associated with MIL-101(Fe), *ex-situ* and *in-operando* XAS experiments are conducted. The two types of XAS results reveal Fe²⁺ relaxation back to the pristine Fe³⁺. To rationalize this phenomenon, electronic structure calculations were conducted to model the side reactions responsible for the lack of reversibility. We propose that the observed Fe²⁺ to Fe³⁺ relaxation promotes irreversible accumulation of lithium in MIL-101(Fe), which leads to the poor capacity retention.

Experimental and Computational Methods

MIL-101(Fe) preparation

MIL-101(Fe) was prepared by using a modified procedure.¹⁸ Equimolar (0.346 mmol) FeCl₃·5H₂O (Sigma Aldrich) and H₂bdc (Sigma Aldrich) were dissolved in 15 mL *N,N*-dimethyl formamide (DMF, Alfa Aesar). This solution was then heated to 150 °C for 15 min via microwave irradiation (CEM discover S-class microwave reactor). After cooling to room temperature, the particles were filtered and washed with 20 mL of DMF and methanol.¹⁸ After washing, the product was dried to evacuate water molecules trapped in the pores. Water can deteriorate the quality of battery electrolyte. Drying was performed at 150 °C under vacuum for 3 h. After the drying process, the product was transferred into a dry glove box (MBraun) filled with high purity Argon (Ar) without exposure to air (Figure S1).

Electrochemical testing

Unless otherwise noted, electrochemical cells were constructed using Swagelok cells with 0.5 inches diameter stainless steel rods as the current collector. Following a previously outlined procedure,¹⁹ assembly was conducted in an Ar filled glove box with Li metal foil (Sigma Aldrich) used as the counter electrode, Whatman GF/D borosilicate glass fiber sheets used as the separators, and 1 M LiPF₆ in 1:1 (by weight) ethylene carbonate:dimethyl carbonate (EC:DMC) (BASF, 1.6 PPM of water) used as the electrolyte. The working electrodes were prepared by ball milling (Retsch PM 100) carbon black (Super-P (SP), Timcal) and MIL-101(Fe) powders in a weight ratio of 3:7, respectively. Specifically, 100 mg total of the powder was milled at 100 rpm for 10 min in a 50 mL agate (Retsch Part # 01.462.0139) jar with a ball to powder weight ratio of 120:1, respectively. Cells were cycled under galvanostatic conditions at room temperature using an Arbin BT 2100 battery tester between the voltages of 2.0 and 3.5 V (versus Li⁺/Li) at rates of C/60, C/40, C/20, and C/10.

Theoretical capacity was calculated assuming the complete one electron redox reaction of the $\text{Fe}^{3+}/\text{Fe}^{2+}$ redox couple.

Powder X-ray Diffraction (PXRD)

Cycled MIL-101(Fe) material used in the PXRD was prepared at a rate of C/40. After cycling was complete, the electrode was recovered from the disassembled Swagelok cell and washed with dimethyl carbonate (DMC). Upon drying in Ar environment, the sample was placed inside a kapton capillary tube and sealed with epoxy glue. Ex situ synchrotron powder diffraction experiments were performed using the monochromated X-rays (0.6661 \AA , $300 \mu\text{m}$ diameter beam size) available at the 1-BM beamline of the Advance Photon (Argonne National Laboratory). The samples were sealed in 0.9 mm diameter polyimide capillaries. Diffraction data were collected using a Perkin-Elmer flat panel area detector (XRD 1621 CN3-EHS) over the d-spacing range 1-50 \AA . The raw images were processed within Fit-2D,²⁰ refining the sample-to-detector distance and tilt of the detector relative to the beam based on the data obtained for a LaB_6 standard.

X-ray Absorption Spectroscopy

In-operando XAS was performed at the Stanford Synchrotron Radiation Lightsource (SSRL) using the fluorescence mode of beamline 4-1. The *in-operando* battery was assembled using a custom designed coin cell with Cirlex film (Fralock) as the X-ray transparent window and cycled at a rate of C/20 during *in-operando* XAS measurements. Transmission mode *ex-situ* XAS experiments were performed at APS 9-BM. Electrode samples were prepared as outlined above for the PXRD samples. After drying, the sample was sealed between two layers of Kapton tape (KaptonTape.com). For both experiments, the XANES (X-ray Absorption Near Edge Spectroscopy) region normalization and the EXAFS

(Extended X-ray Absorption Fine Structure) region Fourier transformation were done using Athena software.²² The extracted EXAFS signals $\chi(k)$, were weighted by k^2 to emphasize the high-energy oscillations and the signals were then Fourier-transformed in a k -range of 2.0 ~ 10.0 \AA^{-1} (*in-operando*) or 2.0 ~ 9.0 \AA^{-1} (*ex-situ*). During the Fourier-transform, a Hanning termination window with a dk value of 1 was utilized to obtain the magnitude plots of the EXAFS spectra in an R -space (\AA).

Computational methods

All calculations were performed with Gaussian 09 (Rev C.01) using the hybrid B3LYP functional with a 10^{-8} convergence criterion for the elements of the density matrix.²³ The fully optimized contracted triple- ζ all-electron Gaussian basis set developed by Ahlrichs and co-workers was employed for all atoms, with the addition of polarization functions for Fe.²⁴ Vibrational analysis was performed for all the optimized structures, and the corresponding harmonic frequencies were used to estimate the thermodynamic quantities. The MIL-101(Fe) secondary building unit was properly modeled for computational efficiency (Figure S2). The different spin topologies were modeled using the fragments option, which allows the definition of specific electronic structures for each metal center. The broken-symmetry solutions were spin-projected by using equation [1], where J is the exchange coupling constant, E_{BS} is the energy of the broken symmetry state, E_{HS} is the energy of the highest spin state, $\langle S^2 \rangle_{BS}$ is the spin expected value of the total spin for the broken symmetry, and $\langle S^2 \rangle_{HS}$ is the spin expected value of the total spin for the highest spin state,

$$J = \frac{2(E_{BS} - E_{HS})}{\langle S^2 \rangle_{HS} - \langle S^2 \rangle_{BS}} \quad [1]$$

Results

Figure 2 presents the electrochemical performance of MIL-101(Fe) electrodes versus Li counter electrodes. Upon initial lithiation (Figure 2a), it was found that MIL-101(Fe) accommodates 0.62 Li/Fe. Compared to previous reports, this value is similar to that of MIL-53(Fe) (~0.62 Li/Fe) and higher than that of MIL-68(Fe) (~0.35 Li/Fe). However, MIL-101(Fe) achieves this value at a higher voltage cutoff of 2.0 V (1.5 V cutoff for MIL-53(Fe) and MIL-68(Fe)). The initial Coulombic efficiency for MIL-101(Fe) is 79%, which is lower than the value previously reported for MIL-53(Fe) (~97%) but close to that measured for MIL-68(Fe) (~79%). Due to this irreversibility, MIL-101(Fe) exhibits poor capacity retention and accommodates only 0.37 Li/Fe by the 5th cycle.

To characterize the electrochemistry of MIL-101(Fe), we studied the differential capacity (dQ/dV) of the first 5 cycles (Figure 2b). During the first cycle, we observed five distinct reduction peaks at 2.99, 2.59, 2.42, 2.27, and 2.13 V as well as two distinct oxidation peaks at 2.87 and 3.00 V. Multiple peaks are expected because MIL-101(Fe) has a complex SBU structure with several different Li insertion sites. A previous computational study found that MIL-53(Fe) has at least two distinct sites available for Li insertion.²⁵ A set of *ex-situ* XAS data suggests that at least two different reactions occurred upon lithiation of MIL-101(Fe) (Figure S3 and Figure S4). Exact assignment of redox peaks to particular lithiation sites is best left to computational studies beyond the scope of this work. In the subsequent cycles, the 2.42 V reduction peak and the 2.87 V oxidation peak increased in intensity while all other peaks reduced in intensity. With extended cycling, it was observed that all oxidation and reduction peaks decreased in intensity (Figure S5). It is noted that the 2.99 V and 2.59 V reductive peaks fade at much different rates. A different rate of degradation indicates that the observed irreversibility MIL-101(Fe) may be associated with a particular Li insertion site.

In order to study how the rate of lithiation/de-lithiation affects reversibility, MIL-101(Fe) cells were cycled for 30 cycles at rates of C/60, C/40, C/20, and C/10 (Figure 2c). Initially, faster rates were associated with lower degrees of lithiation; however, with extended cycling the cells cycled at faster rates exhibited better capacity retention than the cells cycled at slower rates. Specifically, the C/60 cell delivered a 30th cycle discharge capacity of only 0.1 Li/Fe while the C/10 cell delivered a 30th cycle discharge of 0.2 Li/Fe. The C/10 cell delivered a higher 30th cycle discharge capacity in spite of accommodating the least amount of lithium on the first cycle. This result clearly indicated that there is a stability issue with the lithiated state of MOF.

To further investigate the dependency that the rate has upon capacity retention, we studied how incorporating an open-circuit voltage rest into the cycling protocol affects the reversibility of lithium extraction. After being discharged at a rate of C/20, the MIL-101(Fe) cells were rested for 0, 10, 20, 50, or 72 hours and then charged at a rate of C/20. Figure 2d it shows that the percentage of lithium extracted was dependent upon the duration of the rest step. If no rest step was included in the cycling protocol, then the Coulombic efficiency was 73%. However, the Coulombic efficiency was only 23% after a rest of 72 hours. This experiment indicates that lithiated MIL-101(Fe) suffers from an irreversible relaxation mechanism that reduces reversibility.

Like many battery materials, MOFs tend to undergo a conversion reaction if lithiated beyond a certain point. Very often this conversion reaction is irreversible. In the case of MOFs, if the Fe³⁺ is reduced beyond a certain point, this results in the disintegration of the material structure.^{13, 25} Synchrotron PXRD was utilized in order to determine if any significant structural changes occur during cycling which could account for MIL-101(Fe) poor reversibility (Figure 3). A simulated PXRD pattern of MIL-101(Cr) was utilized as a reference.²⁶ MIL-101(Fe) shows some minor secondary phase peaks that are related to

irreversible SP decomposition in the electrochemical cell. In addition, a reversible change in intensity was observed for some peaks including the (022) peak. These changes in intensity are attributed to solvent molecules intercalating along with the Li^+ . Further discussions regarding the secondary phases and the intensities changes are described in the Supporting Information. Most importantly, the irreversible changes in the diffraction patterns were only related to the secondary phase, suggesting that MIL-101(Fe) was stable during cycling and that the poor capacity retention was not due to disintegration of the framework.

In-operando XAS of the Fe K-edge was used to characterize the short range structural changes occurring in MIL-101(Fe) during a full lithiation/de-lithiation cycle at a rate of C/20. In the XAS experiment, MIL-101(Fe) only achieved an initial discharge capacity of 0.3 Li/Fe, whereas in the C/20 experiment without the beam, (Figure 2c) MIL-101(Fe) could achieve an initial discharge capacity of 0.57 Li/Fe at the same rate. We suspect that irradiation of the sample during the *in-operando* XAS measurement contributed to a lower lithium insertion capacity.^{27, 28} Figure 4a presents a contour plot of the XANES region with respect to measurement time where it is observed that the Fe K-edge shifts to lower binding energy during lithiation and then reversibly shifts back to its pristine binding energy upon de-lithiation. A shift to a lower binding energy during lithiation is consistent with the reduction of Fe^{3+} to a mixed valence state of Fe^{3+} and Fe^{2+} . Upon de-lithiation, the mixed valence state is oxidized back to Fe^{3+} . Because the binding energy shift is reversible, *in-operando* XAS also does not explain the poor capacity retention of MIL-101(Fe) (Figure 2d).

Unlike the *in-operando* XAS or PXRD experiments, the results of our *ex-situ* XAS experiment help describe the time dependent capacity fade mechanism. Figure 4b presents a comparison between the *in-operando* and *ex-situ* XANES spectra of MIL-101(Fe) in its pristine, lithiated, and de-lithiated states. The time between electrode preparation and *ex-situ* XAS measurement was 3-4 days. Our first observation was that the spectra intensities near

the Fe K-edge were always lower for the *in-operando* samples. This can be explained by the fact that the *in-operando* samples were thicker than the *ex-situ* samples such that more signal was lost to self absorption.^{29, 30} More importantly, the K-edge of the lithiated *ex-situ* sample did not shift to a lower binding energy as it did for the lithiated *in-operando* sample. This result indicates that the $\text{Fe}^{3+}/\text{Fe}^{2+}$ mixed valence state formed upon lithiation is not stable over longer times. For this reason, the $\text{Fe}^{3+}/\text{Fe}^{2+}$ mixed valence state can be observed only using *in-operando* XAS.

A contour plot of the *in-operando* XAS experiment Fourier transformed EXAFS spectra are provided in Figure 5. The Fourier transform of the EXAFS region is correlated to the radial distribution of nearest neighbor atoms about Fe. The nearest neighbor atoms for Fe are observed at approximately 1.5 Å. In the pristine state, the three Fe ions of the SBU are coordinated with 17 O and one Cl nearest neighbor. The intensity of the spectrum at 1.5 Å decreases upon lithiation and then increases again upon de-lithiation. We attribute the variability of intensity to a reversible change in the coordination environment of the nearest neighbors. Cl⁻ ions are known to be labile³¹ and scatter X-rays more intensely than O²⁻ ions. With this in mind, it may be possible that for each Fe, one O atom from an electrolyte solvent molecule replaces Cl⁻ ion upon full lithiation.

To gain further insight into the EXAFS results, electronic structure calculations on the MIL-101(Fe) SBU were performed. A simplified SBU model (Trimer, Figure S2a) was used in the calculations. Similarly to the model provided in Figure 1a, the SBU model includes the three Fe centers, but replaces the benzene groups with methyl groups in order to reduce the computational cost. An additional model (TrimerDMC, Figure S2b) has been also investigated. In this second model, the axial Cl has been replaced by a carboxylate group, coordinated to the Fe center via one oxygen atom from the carbonyl group. Both models have been used to evaluate the changes in the free energy associated with incremental reduction of

the metal centers.

Because there are different reduction centers in the two models, all possible combinations were calculated (Figure 6 and Table S2). In Figure 6, blue and green dots are used to simply represent the electronic structure of Fe. The calculated free energy of the reduced SBUs was found to be largely independent of the particular Fe center reduced. The first electron reduction of Fe (one green dot, one Fe center reduction $\text{Fe}^{3+}/\text{Fe}^{2+}$) required -3.13 eV for the Trimer model and -6.46 eV for the TrimerDMC model. In all four cases one electron reduction is associated with a negative ΔG indicating that both models strongly prefer to exist in a reduced state. These results indicate that the reduction of the MIL-101(Fe) SBU is twice as favorable when a DMC molecule is coordinated to the iron metal center, and that Cl^- coordination can slow down the reduction process. Furthermore, the second electron reduction (2 green dots, two Fe center reductions $\text{Fe}^{3+}/\text{Fe}^{2+}$) requires -3.36 eV for the Trimer model and -9.00 eV for the TrimerDMC model. In both cases, addition of a second electron provides with further stabilization on the system. However, the reduced TrimerDMC model is much more stable than the Trimer model. This allows us to conclude that substituting Cl^- for a DMC molecule makes the MIL-101(Fe) MOF much more prone to a two electron reduction, results that can be correlated with the changes in the PXRD peak intensities with cycling (Figure 3).

Discussion

Relaxation of Fe^{2+} to Fe^{3+} will result in the irreversible accumulation of Li^+ ions in MIL-101(Fe). As more Li^+ ions accumulate, MIL-101(Fe) loses potential Li^+ ion insertion sites and empty Li^+ site energy drastically increases for future cycles. Computational work on MIL-53(Fe) supports this notion.²⁵ As the sites fill up, the energy required for additional Li^+ insertion will eventually surpass the free energy of Fe^{3+} reduction. It is the constant accumulation of Li^+ ions that cause the capacity of MIL-101(Fe) to rapidly fade.

In addition to the *in-operando* EXAFS, we conducted an *ex-situ* EXAFS experiment (Figure S3 and S4). *Ex-situ* EXAFS spectra were collected after the MIL-101(Fe) MOF electrode was reduced to 2.5 V and again after the electrode was further reduced to 2.0 V. Although the first neighbor peak intensity was identical for the pristine and the 2.5 V sample, there is a reduction in the first neighbor peak intensity for the 2.0 V sample. When the electrode was oxidized back to 3.5 V, the first neighbor peak did not completely regain intensity. The *ex-situ* EXAFS data thus provide further support for our computational results suggesting that Cl^- ions may be irreversibly replaced by DMC molecules in order to decrease the free energy of Fe site reduction.

A major point provided from the electronic structure calculations is the significant difference observed in the free energy profiles associated to the changes in the axial coordination sphere of the iron metal center. Different coordination spheres lead to different behaviors towards reduction, thus affecting the recycling efficiency of the material. Because a Cl^- ion can be more easily detached from the coordination sphere. As observed in Figure 2d, a longer rest time between the lithiation and de-lithiation reduces the coulombic efficiency. This temporal effect can be associated with Cl^- ligand lability. After lithiation, the Cl^- ligand can dissociate from the Fe center, and with longer times, the anion can diffuse further away from the metal center. This may have detrimental effects on the electrochemical performance

since MIL-101(Fe) will not regain its pristine structure after de-lithation. One way to try to avoid such irreversible change is to switch Cl^- to F^- to strengthen the bond between Fe-F. However this will require the use of HF. Other possible ways to improve the reversibility of the MIL-101(Fe) redox would be to improve the stability of its reduced SBU. To stabilize the SBU, one can alter the electronic structure of SBU. Many studies have demonstrated different pathways to alter the electronic structure via ligand functionalization,³⁵ by increasing the conjugation on the system.⁹ In addition, one can replace the ligands with other redox active organic molecules such as benzoquinones,³² organic radicals,^{8, 33, 34} or oxocarbons.³⁵

Conclusions

In this work, the MIL-101(Fe) MOF was tested as an electrode for use in lithium ion batteries. The redox chemistry ($\text{Fe}^{2+}/\text{Fe}^{3+}$) was found to not be completely reversible. We characterized the decay mechanism using *ex-situ* and *in-operando* XAS measurements. The Fe^{2+} oxidation state was not observed from *ex-situ* experiments. The temporal dependency of Fe^{2+} observation indicates the importance of *in-operando* experiments. The computational results indicate that significant energy differences can be expected between the pristine and reduced forms of MIL-101(Fe). This is ascribed to the axial ligand coordinated to the Fe^{3+} metal centers. Our study thus suggests that an appropriate functionalization of the MIL-101(Fe) SBUs can improve the reversibility of the $\text{Fe}^{2+}/\text{Fe}^{3+}$ redox reaction.

Acknowledgements

This work is supported by the University of California, San Diego's Chancellor's Interdisciplinary Collaboratories program. Use of the Advanced Photon Source, an Office of Science User Facility operated for the U.S. Department of Energy (DOE) Office of Science by Argonne National Laboratory, was supported by the U.S. DOE under Contract No. DE-AC02-06CH11357. The theoretical and computational analyses were supported by the National Science Foundation (Award Number DMR-1305101 to F.P.) and used resources of the Extreme Science and Engineering Discovery Environment (XSEDE), which is supported by the National Science Foundation Grant Number OCI-1053575 (Allocation TG-CHE110009 to F.P.). MOF synthesis was also supported by a grant from the Department of Energy, Office of Basic Energy Sciences, Division of Materials Science and Engineering under Award No. DE-FG02-08ER46519 (S.M.C.). The authors would also like to thank Prof. Eric Fullerton at UCSD for the access to magnetic susceptibility measurements.

Figures

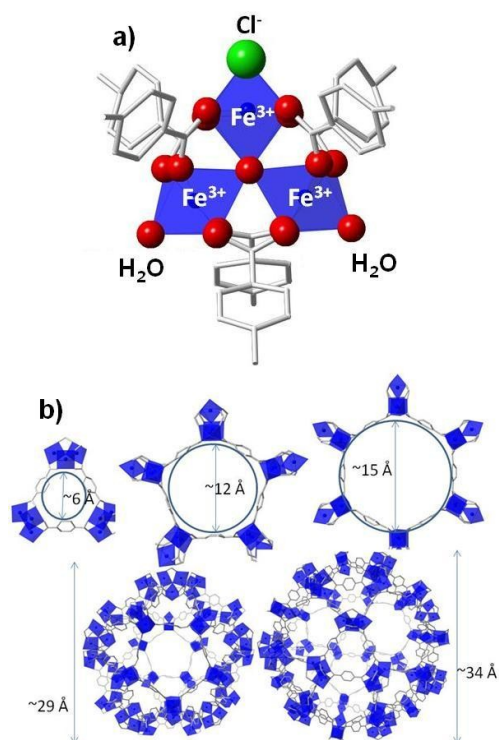


Figure 1: Structure of MIL-101(Fe). a) The SBU (blue, Fe; red, O; stick, C; green, Cl; H is omitted for clarity). b) The windows and pores of MIL-101(Fe) with Cl and O atoms omitted for clarity.

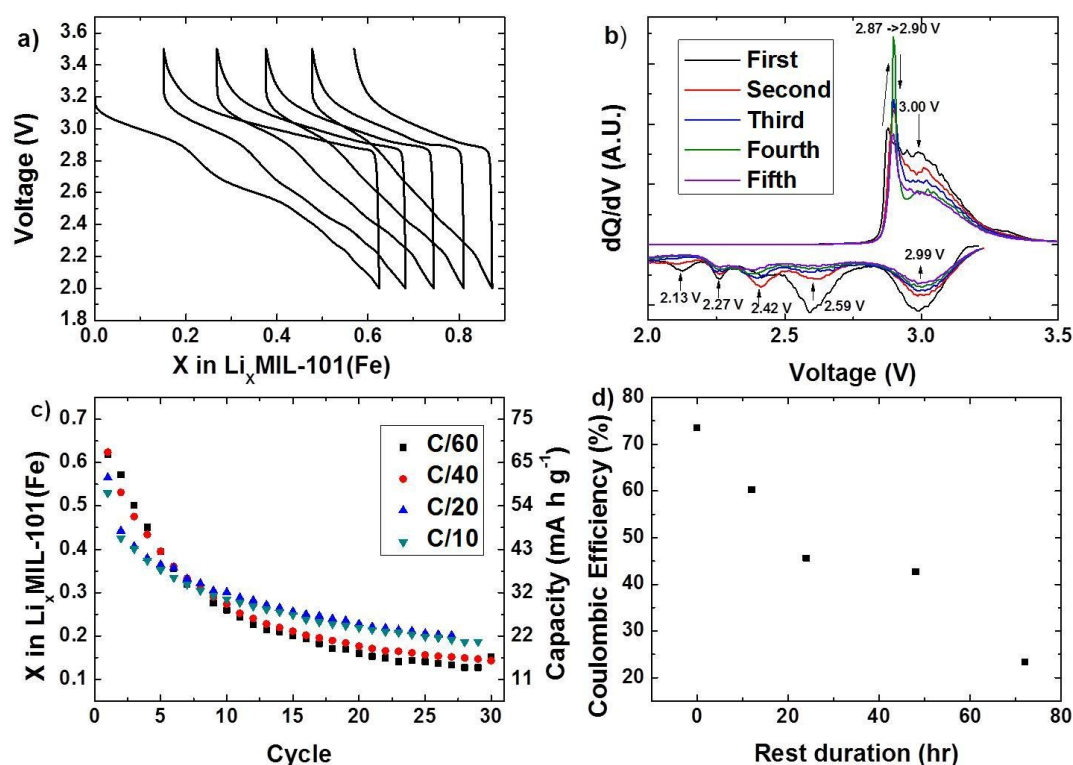


Figure 2: Results of galvanostatically cycling MIL-101(Fe) electrodes versus a Li counter electrode. a) First five voltage profiles at a rate of C/40. b) Differential capacity (dQ/dV) of the first 5 cycles at a rate of C/40. c) Cyclic capacity of MIL-101(Fe) electrodes at a variety of different C-rates. d) First cycle Coulombic efficiency of MIL-101(Fe) electrodes which were rested between discharge (C/20) and charge (C/20) for different amounts of time. Coulombic efficiency decreases as the rest time is increased.

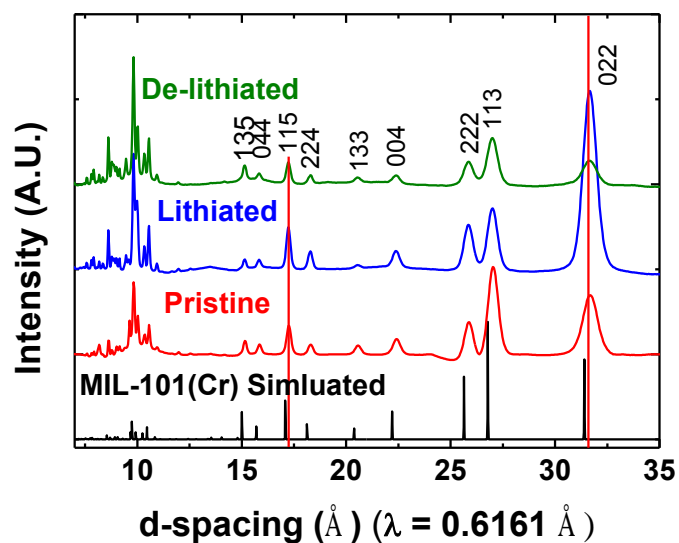


Figure 3: Synchrotron PXRD patterns for MIL-101(Fe) prior to cycling (red), after lithiation (blue), and after de-lithiation (green). Patterns are compared to a simulated pattern of the MIL-101(Cr) analogue structure. Red lines indicate peaks that show a reversible change in intensity.

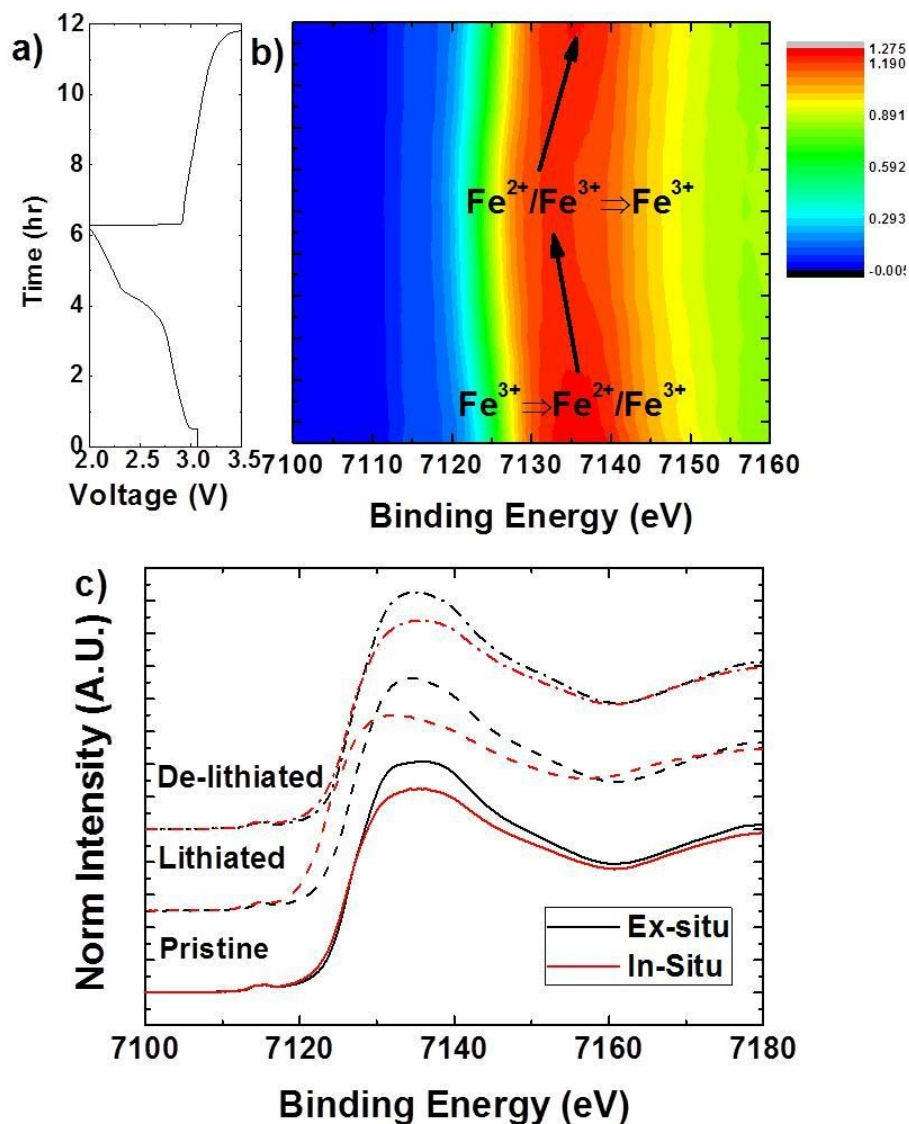


Figure 4: *In-operando* and *ex-situ* XANES of MIL-101(Fe). a) Voltage profile with respect to the *in-operando* XAS scanning time. b) The contour plot of the *in-operando* XAS XANES region versus time indicates a reversible change in the Fe oxidation state. c) Comparison of the *in-operando* (red) and *ex-situ* (black) XAS XANES spectra. The Fe K-edge of the *ex-situ* lithiated sample does not shift to a lower binding energy that indicates the presence of a time dependent fade mechanism.

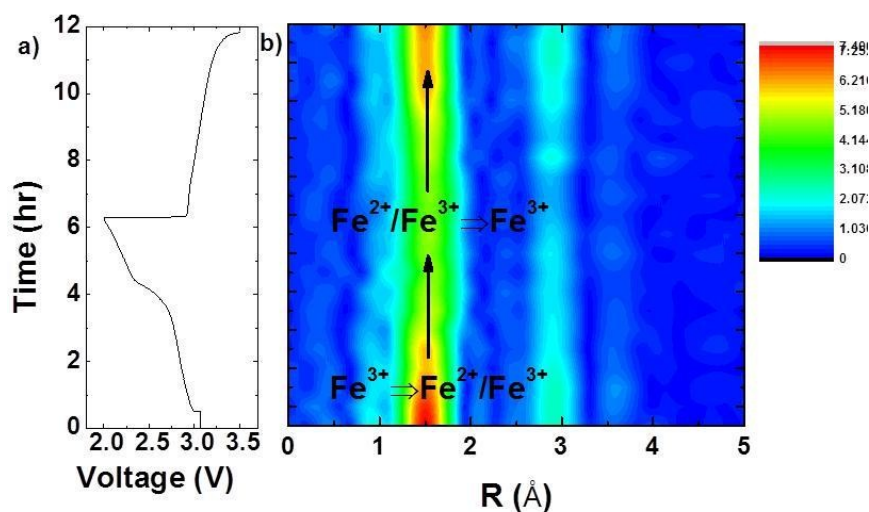


Figure 5: Fourier transformed EXAFS region of the *in-operando* XAS data. a) Voltage profile with respect to the *in-operando* XAS scanning time. b) Contour plot of the EXAFS region versus time that indicates a reversible change in Fe coordination during cycling.

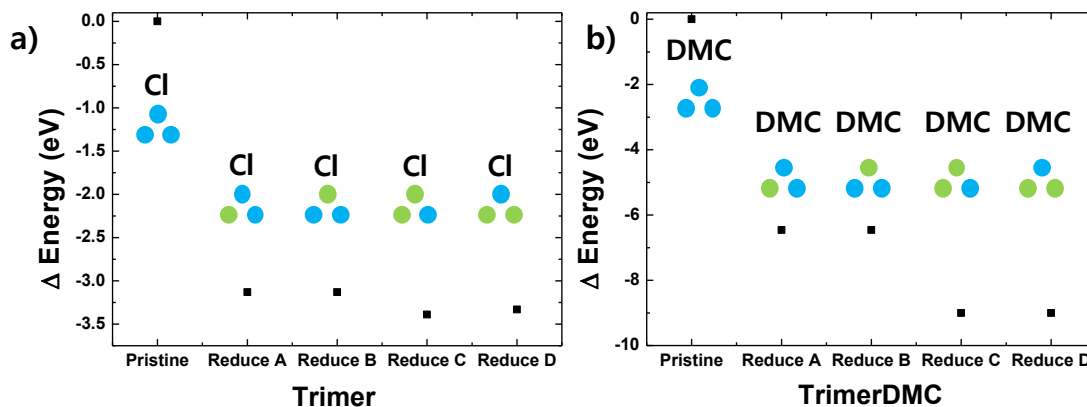


Figure 6: Gibbs free energies relative to the respective pristine state are shown for the a) Trimer and b) TrimerDMC model and its reduced forms. Insets: Oxidation state of Fe for the respective reduced states are illustrated in simple dots. Blue dots are Fe^{3+} and green dots are Fe^{2+} .

References

1. M. Armand and J. M. Tarascon, *Nature*, 2008, 451, 652-657.
2. F. S. Anthony, *Journal of Chemical Education*, 1983, 60.
3. J. Tarascon and M. Armand, *Nature*, 2001, 414, 359-367.
4. J.-M. Tarascon, *ChemSusChem*, 2008, 1, 777-779.
5. J. M. Pearce, *International Journal of Nuclear Governance, Economy and Ecology*, 2008, 2, 17.
6. W. Walker, S. Grugeon, O. Mentre, S. Laruelle, J. M. Tarascon and F. Wudl, *Journal of the American Chemical Society*, 2010, 132, 6517-6523.
7. W. Walker, S. Grugeon, H. Vezin, S. Laruelle, M. Armand, J. M. Tarascon and F. Wudl, *Electrochemistry Communications*, 2010, 12, 1348-1351.
8. K. Nakahara, S. Iwasa, M. Satoh, Y. Morioka, J. Iriyama, M. Suguro and E. Hasegawa, *Chem Phys Lett*, 2002, 359, 351-354.
9. S. E. Burkhardt, J. Bois, J. M. Tarascon, R. G. Hennig and H. D. Abruna, *Chem Mater*, 2013, 25, 132-141.
10. J. Kim, B. L. Chen, T. M. Reineke, H. L. Li, M. Eddaoudi, D. B. Moler, M. O'Keeffe and O. M. Yaghi, *Journal of the American Chemical Society*, 2001, 123, 8239-8247.
11. C. Mellot-Draznieks, J. Dutour and G. Férey, *Z Anorg Allg Chem*, 2004, 630, 2599-2604.
12. L. Xiaoxia, C. Fangyi, Z. Shuna and C. Jun, *Journal of Power Sources*, 2006, 160.
13. G. Férey, F. Millange, M. Morcrette, C. Serre, M.-L. Doublet, J.-M. Grenèche and J.-M. Tarascon, *Angewandte Chemie (International ed. in English)*, 2007, 46, 3259-3263.
14. F. Alexandra, H. Patricia, D. Thomas, S. Christian, M. Jérôme, G. Jean-Marc, M. Mathieu, T. Jean-Marie, M. Guillaume and F. Gérard, *European Journal of Inorganic Chemistry*, 2010, 2010.
15. J. Overgaard, F. K. Larsen, B. Schiott and B. B. Iversen, *Journal of the American Chemical Society*, 2003, 125, 11088-11099.
16. A. K. Dutta, S. K. Maji and S. Dutta, *J Mol Struct*, 2012, 1027, 87-91.
17. A. K. Boudalis, Y. Sanakis, F. Dahan, M. Hendrich and J. P. Tuchagues, *Inorg Chem*, 2006, 45, 443-453.
18. K. Taylor-Pashow, J. Della Rocca, Z. Xie, S. Tran and W. Lin, *Journal of the American Chemical Society*, 2009, 131, 14261-14263.
19. G. Férey, F. Millange, M. Morcrette, C. Serre, M. L. Doublet, J. M. Grenèche and J. M. Tarascon, *Angew Chem Int Edit*, 2007, 46, 3259-3263.
20. A. P. Hammersley, *ESRF Internal Report*, 1997, ESRF97HA02T.
21. A. P. Hammersley, Svensson, S. O., Hanfland, M. Fitch, A. N., & Häusermann, D. , *High Pressure Res*, 1996, 14, 235-248.
22. B. Ravel and M. Newville, *Journal of synchrotron radiation*, 2005, 12, 537-541.
23. A. D. Becke, *J Chem Phys*, 1993, 98, 5648-5652.
24. A. Schafer, C. Huber and R. Ahlrichs, *J Chem Phys*, 1994, 100, 5829-5835.

25. C. Combelles, M. Ben Yahia, L. Pedesseau and M. L. Doublet, *J Phys Chem C*, 2010, 114, 9518-9527.
26. G. Férey, C. Mellot-Draznieks, C. Serre, F. Millange, J. Dutour, S. Surble and I. Margiolaki, *Science*, 2005, 309, 2040-2042.
27. S. V. Antonyuk and M. A. Hough, *Bba-Proteins Proteom*, 2011, 1814, 778-784.
28. J. Qiu, L. Cao, P. Mulligan, D. Turkoglu, S. C. Nagpure, M. Canova and A. Co, *Ieee T Nucl Sci*, 2013, 60, 662-667.
29. E. A. Stern and K. Kim, *Phys Rev B*, 1981, 23, 3781-3787.
30. C. H. Booth and F. Bridges, *Phys Scripta*, 2005, T115, 202-204.
31. Y. P. Ou, D. Feng and J. J. Yuan, *Acta Crystallogr E*, 2010, 66, M921-U558.
32. T. Le Gall, K. H. Reiman, M. C. Grossel and J. R. Owen, *Journal of Power Sources*, 2003, 119, 316-320.
33. J. Q. Qu, T. Katsumata, M. Satoh, J. Wada and T. Masuda, *Macromolecules*, 2007, 40, 3136-3144.
34. H. Nishide, S. Iwasa, Y. J. Pu, T. Suga, K. Nakahara and M. Satoh, *Electrochimica Acta*, 2004, 50, 827-831.
35. H. Chen, M. Armand, G. Demailly, F. Dolhem, P. Poizot and J. M. Tarascon, *ChemSusChem*, 2008, 1, 348-355.